Comprehensive analysis of the green to blue photoconversion of full-length cyanobacteriochrome Tlr0924

Samantha J. O. Hardman,[†] Anna F. E. Hauck,[†] Ian P. Clark,[‡] Derren J. Heyes,[†] Nigel S. Scrutton[†]*

[†]Manchester Institute of Biotechnology and Photon Science Institute, Faculty of Life Sciences, University of Manchester, 131 Princess Street, Manchester M1 7DN, UK

[‡] Central Laser Facility, Research Complex at Harwell, Science and Technology Facilities Council, Harwell Oxford, Didcot, OX11 0QX, UK

S. J. O. Hardman and A. F. E. Hauck contributed equally to this work.

* Correspondence: nigel.scrutton@manchester.ac.uk

ABSTRACT

Cyanobacteriochromes are members of the phytochrome superfamily of photoreceptors and are central in biological light activated signalling mechanisms. These photoreceptors are known to reversibly convert between two states in a photoinitiated process which involves a basic *E/Z* isomerisation of the bilin chromophore, and in certain cases the breakage of a thioether linkage to a conserved cysteine residue in the bulk protein structure. The exact details and timescales of the reactions involved in these photoconversions have not been conclusively shown. The cyanobacteriochrome Tlr0924 contains phycocyanobilin and phycoviolobilin chromophores, both of which photoconvert between two species, blue-absorbing and green-absorbing, and blue-absorbing and red-absorbing, respectively. Here we have followed the complete green to blue photoconversion process of the phycoviolobilin chromophore in the full-length form of Tlr0924 over timescales ranging from femtoseconds to seconds. Using a combination of time-resolved visible and mid-IR transient absorption spectroscopy and cryotrapping techniques we have shown that after photoisomerisation, which occurs with a lifetime of 3.6 ps, the phycoviolobilin twists, or distorts slightly with a lifetime of 5.3 μs. The final step, the formation of the thioether linkage with the protein occurs with a lifetime of 23.6 ms.

INTRODUCTION

The photochemically versatile class of proteins known as cyanobacteriochromes (CBCRs) mediate a variety of molecular outputs *via* the reversible *E/Z* isomerisation of a sensory bilin chromophore in their cyanobacterial host organism.(1) The general protein structure is divided into domains, always including the photosensory chromophore binding GAF (cGMP-specific phosphodiesterase / adenylyl cyclase / FhlA protein) domain in the N-terminus and an output domain (e.g., histidine kinase or GGDEF domain) in the C-terminus.(1, 2) There is great functional versatility in different subgroups of the protein class. Modifications of the central chromophore also permit a collective spanning of the entire UV/Vis spectrum.(1, 3, 4) CBCRs have attracted a great deal of attention as novel photoreceptors. Variations in domain architecture and chromophore structure permit creation of proteins of a specific function for applications such as fluorescence biomarking,(5) optogenetics,(6) and the production of biofuels.(7) At the heart of these developments is a thorough understanding of the protein as a photoreceptor.

Photochemical reactions of biological molecules are frequently fast and efficient. CBCRs and the related phytochromes and bacteriophytochromes have increasingly been characterized on femtosecond to nanosecond timescales.(8-13) In general terms, both the 'forward' *Z/E* isomerisation and 'reverse' *E/Z* isomerisation of the chromophore usually occur within several hundred ps.(10, 13, 14) This induces further structural changes, manifested in the form of mostly unknown intermediate structures,(15-17) ultimately leading to protein conformational changes to activate the output domain. The CBCR Tlr0924 from *Thermosynechococcus elongatus* is a photoreceptor from the DXCF subgroup (containing the Asp-Xaa-Cys-Phe motif) of CBCRs which has been the focus of a number of studies,(18-21) and has recently been found to regulate sessility *in vivo*.(22) Heterologously expressed Tlr0924 incorporates a red-absorbing (Pr) phycocyanobilin (PCB) chromophore through covalent linkage between Cys527 and the ethylidene side chain of ring A (Fig. 1).(21) On a timescale of days autoisomerase activity of the GAF domain subsequently converts ~80 % of the PCB population to a phycoviolobilin (PVB) population.(23, 24) PVB is saturated at the C5 position, between rings A and B, and hence the π-conjugated system is restricted to rings B-D to yield a green-absorbing species (Pg). The *15Z* isomers of PVB and PCB can form a second covalent linkage between Cys499 and the C10 position, between rings B and C, to form species PVB' and PCB' respectively. This second Cys linkage shortens the π-conjugation to rings C and D only in both chromophores, yielding identical blue-absorbing dark states (Pb). After photoconversion to the Pg or Pr states reversion to the dark Pb states typically occurs slowly, over several hours.(3, 23) The combination of chromophores means that Tlr0924 is photosensitive to virtually the entire visible spectrum (Fig. 1). Characterization of the various photostates involved has been carried out using acid denaturation and selective sequential photoconversion.(21, 23) If Tlr0924 containing a mixture of PVB' and PCB' is illuminated with blue light, conversion will occur from both (spectrally identical in the visible region) Pb states. When the sample is then illuminated with red light only the PCB Pr state will convert back to the Pb state. When green light is used both the PVB and PCB populations will be returned to their respective Pb states.
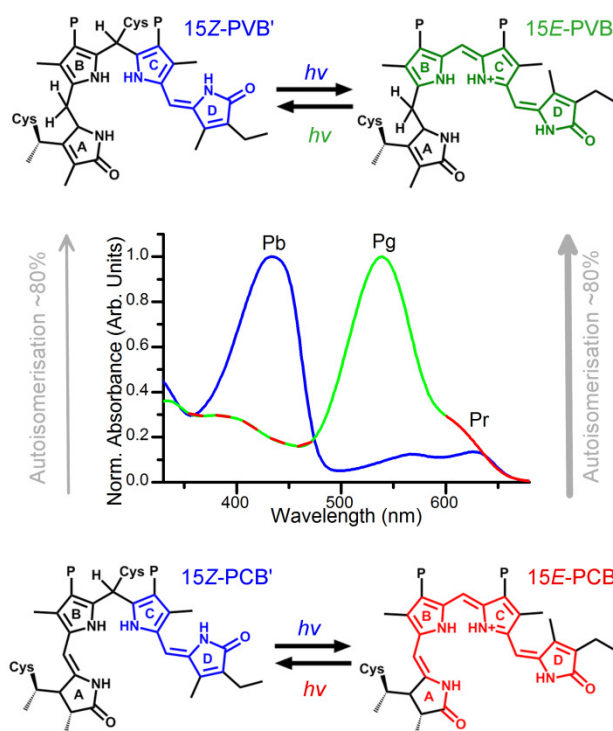
FIGURE 1 Structures and absorption spectra of the PCB and PVB photostates. The PCB and PVB chromophores can interconvert by autoisomerization, the ^{15Z}Pb and ^{15E}Pg and ^{15E}Pr states can reversibly photoconvert.

A description of the complete 'forward' photoconversion for the full-length protein has recently been published.(20) The only previous time-resolved study of the reverse photoreaction of Tlr0924 was of the fs-ns photoisomerisation dynamics of the GAF domain protein.(18) Here we use a combination of time-resolved spectroscopies covering fs to s timescales, and cryotrapping measurements to comprehensively characterize the 'reverse' photoreaction of the dominant PVB chromophore in full length Tlr0924.

MATERIALS AND METHODS

Protein expression and purification

Full-length Tlr0924 was expressed and purified as described previously.(20) The sample was dissolved in a phosphate based buffer system (100 mM sodium-potassium phosphate, 300 mM NaCl, pH 7). UV/Vis spectroscopy was used to determine the relative PVB:PCB chromophore ratio as approximately 80% PVB and 20% PCB. This ratio was assumed to remain constant over the course of the experiments.(25)

Ultrafast transient absorption spectroscopy

The 1 kHz repetition rate laser system used to pump the broad band pump-probe visible transient absorbance spectrometer 'Helios' (Ultrafast Systems LLC, Sarasota, FL) has been previously described.(20) The pump beam was centred at 530 nm with a full width at half maximum intensity of ~50 nm. Excitation energies of 0.6 µJ were used which yielded pump

fluences of 3.4 mJ/cm^2. To maximise the accessible region of the spectrum the polarisation of pump and probe were adjusted to be perpendicular, and a polarizer before the detectors was used to eliminate a large proportion of the scattered pump light. Data collected with a depolarized pump beam (see Fig. S1 in the Supporting Material) yielded kinetics and spectra similar to those shown in Fig. 2, thus we assume any polarization effects will not affect the model derived from these data. The time resolution of the experiment was ~0.2 ps, data points were collected randomly over the 3 ns time frame. Samples were contained in stirred 2 mm pathlength quartz cuvettes (optical density (OD) at 535 nm = 0.5). During the measurements the samples were continuously illuminated through the appropriate bandpass filter (Andover Corp, Salem, NH) using a cold light source (KL1500, Schott, Stafford, UK). Illumination at 435 nm was used to regenerate the PVB and PCB Pr and Pg states from their corresponding Pb states, and simultaneous 640 nm illumination used to regenerate the PCB Pb state from the Pr state, this left only the PVB Pg state to be excited by the pump laser.

Time-resolved IR spectroscopy was carried out at the Ultra facility (CLF, STFC Rutherford Appleton Laboratory, UK), which uses a 10 kHz repetition rate laser and has a time resolution of around 100 fs.[26] Samples dissolved in D$_2$O based phosphate buffer (at the same concentration and equivalent pD as the H$_2$O buffer used in the visible measurements) were flowed through a 100 μm pathlength CaF$_2$ measurement cell (Harrick Scientific, Pleasantville, NY) and the sample holder was rastered in the two dimensions orthogonal to the pump and probe beams to avoid sample damage. The sample was concentrated by a factor of around 20 times compared to that used in the visible measurements so that the OD at 535 nm was ~0.5. An excitation energy of 1 uJ at 530 nm was used, the pump beam diameter was around 150 μm, yielding a fluence of 7.2 mJ/cm^2. The excitation beam was set at the magic angle with respect to the IR probe beam. The Pg state of the sample was regenerated by continuous sample illumination with a cold light source as described above. The spectral resolution was ~3 cm^{-1}, pixel to wavenumber calibration was performed as described previously.[27]

Laser flash photolysis

The laser flash photolysis experimental set up has been described in detail elsewhere.[20] For measurements on sub-ms timescales the probe beam was pulsed and kinetic traces recorded on a digital oscilloscope (Infiniium, 54830B, Agilent Technologies, Santa Clara, CA). Measurements on longer timescales were recorded using a photomultiplier tube. The 532 nm pump pulse duration was 6-8 ns and energies of 26–100 mJ were used (depending on the set of measurements). The beam diameter was on the order of 1 cm, yielding pump fluences of 33–128 mJ/cm^2. The 300–700 nm region was monitored by recording absorption transients in 5 nm steps, each data point being the average of ≥3 transients. The PVB Pg photostate was regenerated after each shot by illumination with a cold source lamp fitted with the relevant bandpass filters. Illumination at 435 nm was used to regenerate the PVB and PCB Pr and Pg states from their corresponding Pb states, and this was followed by 640 nm illumination which regenerated the PCB' Pb state from the Pr state. This left only the PVB Pg state to be excited by the pump laser. The sample was contained in a 1 cm pathlength quartz cuvette and maintained at 25°C by a circulating water bath. The sample had an OD of 0.5 at the excitation wavelength. Samples were frequently replaced and their quality monitored by UV/Visible Spectroscopy (Cary 50, Agilent Technologies).

Cryotrapping

Samples were prepared in the PVB Pg photostate as described above, with an OD at 435 nm of ~ 1 in cryogenic buffer (100 mM sodium-potassium phosphate, 300 mM NaCl, pH 7 aqueous buffer system made using 30% glycerol and 48% sucrose) and cooled to 99 K in a cryochamber (Optistat DN liquid nitrogen cryostat, Oxford Instruments Inc., Abingdon, UK). After recording a UV/Visible reference spectrum (Cary 50, Agilent Technologies) at 99 K the sample was illuminated at 127 K for 10 minutes before being cooled back to 99 K. The sample was then warmed up to 297 K in 10 K steps, at each point the sample equilibrated for ~10 minutes before the sample was cooled to 99 K and a UV/Visible absorbance spectrum recorded. A temperature of 127 K was chosen as the illumination temperature because this was the point at which the ground state bleach feature reached a maximum intensity in a set of benchmarking experiments where the sample was warmed from 77 K in 10 K steps, illuminating at each temperature for 10 minutes before cooling to 77 K to record the spectrum (see Fig. S2 in the Supporting Material).

Global analysis

The transient absorption and laser flash photolysis 3D data-sets were analyzed globally using the open-source software *Glotaran*.(28) This procedure reduces the matrix of time, wavelength, and change in absorbance to one or more exponentially decaying time components, each with a corresponding difference spectrum. The visible and IR ultrafast transient absorption data were fitted from 0.3 and 0.2 ps, respectively to avoid any contributions from coherent artifacts.(29)

RESULTS AND DISCUSSION

Ultrafast Transient Absorption

To isolate the initial photoreaction of the PVB chromophore in Tlr0924 samples were illuminated simultaneously with constant blue and red light and excited with a ~530 nm pulsed laser as described in the methods section. The autoisomerization of chromophores in Tlr0924, which occurs on a timescale of days, results in an approximate PVB:PCB ratio of 4:1.(24) The comparatively small population of the PCB chromophore combined with the selective wavelength constant illumination allows almost complete isolation of the PVB photodynamics. The ultrafast transient absorption (TA) data collected for the initial steps of the PVB photoconversion are shown in Fig. 2a. Within the time resolution of the experiment (0.2 ps) two major spectral features appear: a large negative feature at ~530 nm, which can be assigned to the ground state bleach (GSB) of the Pg state, and a positive features at ~670 nm, which can be assigned to excited state absorption (ESA) of the Pg state. Within 5 ps these features have decayed almost completely, although they are all still distinguishable and a positive feature at ~550 nm appears (see Fig. S3 in the Supporting Material). Global analysis was carried out to more accurately define the spectral intermediates and the timescales of interconversion between intermediate states (Fig. 2b). A model with 4 sequentially converting spectral components, the evolution associated difference spectra (EADS), was found to be a good fit to the data (see Fig. S4 in the Supporting Material) and broadly agreed with literature values for GAF domain only Tlr0924.(18) There was also an obvious contribution from a negative feature at ~645 nm (see Fig. S5 in the Supporting Material) which has previously been ascribed to inactive or modified protein.(20, 21)
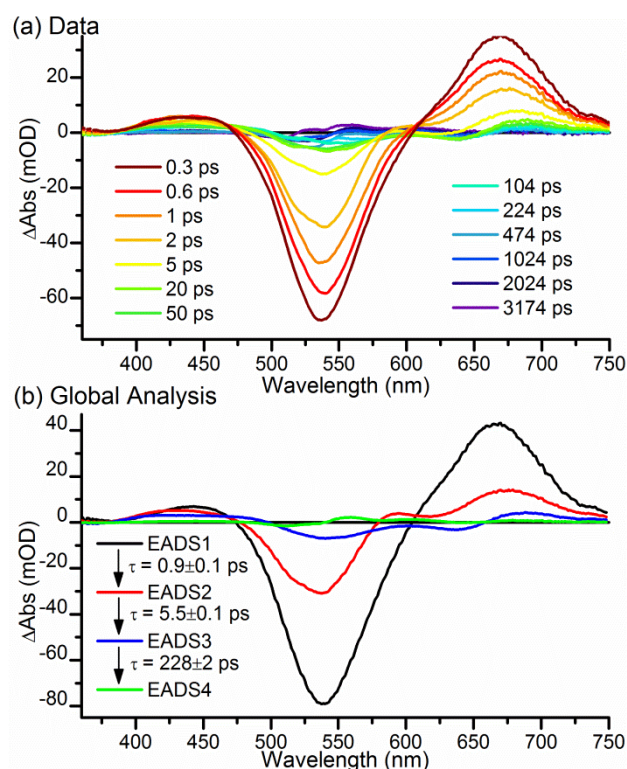
FIGURE 2 Ultrafast visible transient absorption spectra at selected time points (a), and the EADS resulting from a sequential global analysis of the data (b). The sample was constantly illuminated during data collection with blue and red light so the signals primarily originate from the Pg to Pb photoconversion of the PVB chromophore.

The ultrafast IR TA data were collected over the same time range, using the same time steps as were used for the visible TA experiments. The data, shown in Fig. 3a, display a relatively simple picture. There are 3 major negative features at 1402, 1606, and 1685 cm^{-1}, but no immediately apparent positive features. Similar phytochromes have been extensively studied in the mid-IR region, allowing assignment of the 1606 and 1685 cm^{-1} bleaches as C=C stretches in rings A and B,[30, 32] and C=O stretches in ring D,[33, 34] respectively. Global analysis of the data-set using a basic sequential model yields time constants comparable to those found from the visible TA data (Fig. 3b). One fewer component is required to fit the data, and the resulting time constants are 3.6, 196, and 'infinite' ps.
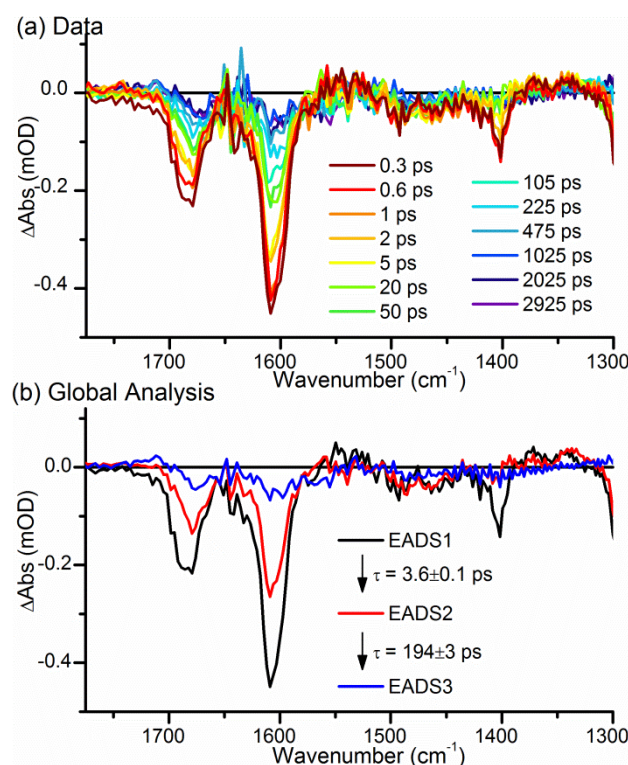
FIGURE 3 Ultrafast IR transient absorption spectra at selected time points (a), and the EADS resulting from a sequential global analysis of the data (b). The sample was constantly illuminated during data collection with blue and red light so the signals primarily originate from the Pg to Pb photoconversion of the PVB chromophore.

To more accurately model the ultrafast processes that occur upon photoisomerisation a more complex global analysis was performed (Fig. 4) to produce species associated difference spectra (SADS). The model was selected after many iterations because it was the model which not only isolated the negative feature at ~645 nm, but also resulted in very comparable lifetimes between the visible and IR data-sets. In this model SADS1 evolves into non-decaying component SADS2. Independently and in parallel to this process SADS3, representing the inactive protein, decays back to the ground state. In the case of the visible TA data an additional lifetime representing SADS1 decaying to the ground state was also fitted. The lifetimes produced by this model correlate extremely well between the visible and IR TA data-sets. The SADS1 to SADS2 conversion lifetime was 3.6±0.1 ps in both data-sets. The lifetime of SADS3 was fitted as 185±2 ps and 194±2 ps for the visible and IR TA data respectively. In the analysis of the visible TA SADS1 was found to relax to the ground state with a lifetime of 0.6±0.1 ps. This component was not resolved in the IR TA data, likely due to the similarity of the excited state and ground state vibrational spectra, with the poor signal-to-noise ratio of these data playing a role. The poor signal-to-noise ratio was due to both the low volume sample and the air bubbles in the sample, unavoidable due to the high flow rate necessary to avoid sample damage during the measurements.
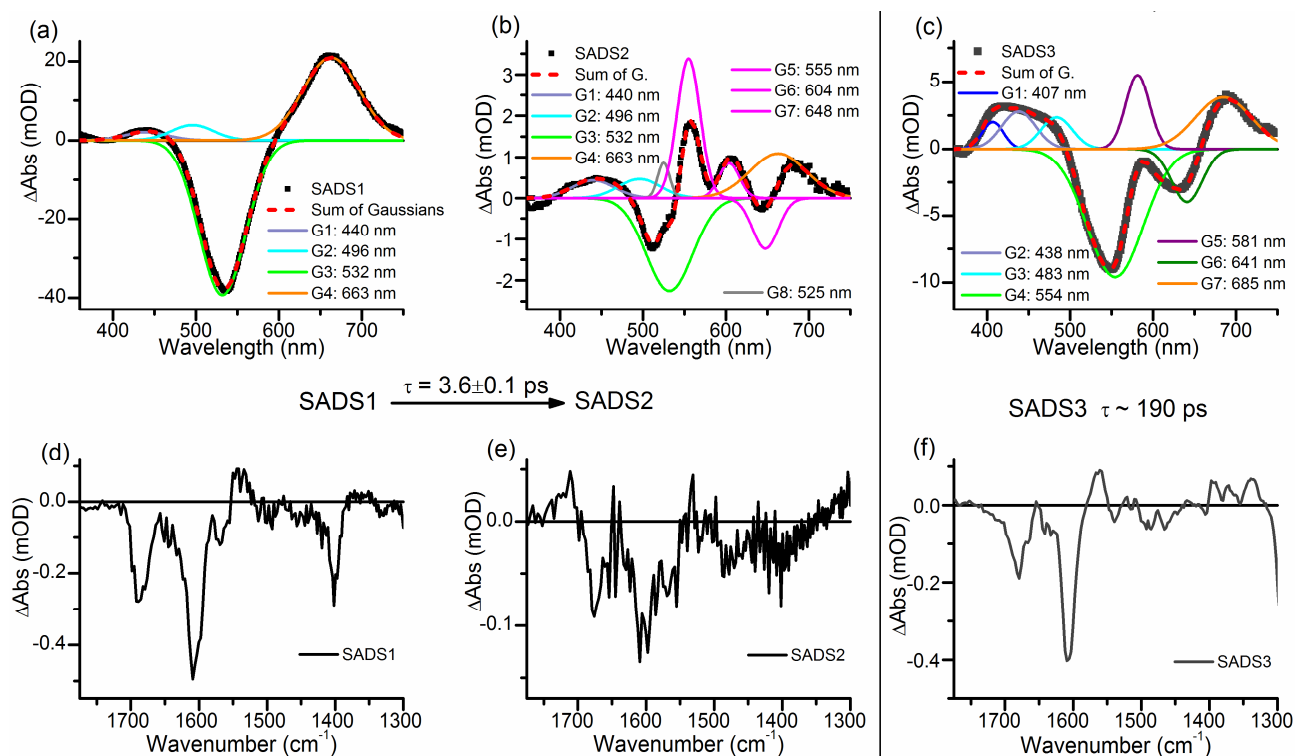
FIGURE 4 Global analysis of the ultrafast visible (a-c) and IR (d-f) transient absorption data showing resulting SADS (black). The visible TA SADS are fitted with a sum of Gaussian functions (dashed red). The features of SADS1 (a) and SADS2(b) are assigned as: GSB of the PVB Pg state at 532 nm (green), ESA features at 440, 496, and 663 nm (lilac, cyan and orange), intermediate states at 550, 604, and 648nm (pink), and pump scatter at 525 nm (grey). SADS3, representing inactive or modified protein has additional peaks at 641 nm (dark green) and 581 nm (purple).

A combination of Gaussian peaks were fitted to the SADS resulting from the visible TA data (Fig. 4a-c). Although it has been shown that bilin chromophores do not have pure Gaussian lineshapes, the use of these functions can provide useful insight into which species are present in each spectrum.(35, 36) SADS1 is very similar in shape to the difference spectra collected at 0.3 ps after excitation. Features corresponding to the PVB Pg GSB centred at 532 nm, as well as ESA features at 440, 496, and 663 nm are clearly defined. The lack of any other negative features in this spectrum is consistent with excitation of only the Pg state, not of any intermediate states that may be present after 1 ms (the separation of pulses in the 1 kHz laser system). These features remain in SADS2 which displays an additional positive feature, which we ascribe to the first reaction intermediate at 555 nm. There are also less intense components at 525, 604, and 648 nm, which may be 'real' features, but are more likely to be artefacts from scattered pump light, residual signal from the 'inactive' protein, and the very low signal levels. SADS3 decays in parallel to the SADS1 to SADS2 conversion and has features similar, although not identical, to SADS1 and SADS2 at 407, 438, 483, 554, 581 and 685 nm. The most significant difference is the large negative feature at 641 nm, corresponding to inactive or modified protein as observed previously.(20) This feature does not correspond to any known state of PCB or PVB in Tlr0924,(23) and various other PCB containing CBCRs show features in this spectral region,(16, 37) suggesting that it is a variation in the GAF domain which produces this red-shifted, inactive population of the protein. This population may account for some of the spectral density above 600 nm in the Pb

absorption spectrum shown in Fig. 1.The SADS resulting from analysis of the IR TA data support the species assignments of the visible TA analysis. SADS1 displays the 3 major bleach peaks observed in the raw data. In addition to the features observed in SADS1 there is a small, but significant positive feature at ~1711 cm^{-1} in SADS2. This correlates well with ultrafast IR TA measurements on the forward photoconversion of PVB' from the Pb state where, shortly after photoexcitation a downshift was observed in the same C=O stretching feature, from ~1700 to ~1686 cm^{-1}, which is assigned to the isomerisation reaction.[20] In parallel to the SADS1 to SADS2 conversion, SADS3 decays with a lifetime of 194 ps. This spectrum confirms the assignment of this independently decaying component as a structurally modified version of the protein. While SADS1 and SADS2 do appear similar SADS3 completely lacks the bleach at ~1402 cm^{-1} , and the C=O stretching feature at ~1686 cm^{-1} in SADS1 appears to have downshifted to ~1680 cm^{-1}.

Nanosecond to Millisecond Transient Absorption

Laser flash photolysis was used to monitor the slower processes occurring in the photoinitiated reaction. By illuminating the entire sample with blue light, to produce the Pg and Pr states, then illuminating with red light it was possible to completely isolate the Pg species. To cover the ns to ms time range two sets of measurements were performed, from 20 ns to 8 μs, and from ~1 μs to 450 μs. From the data shown in Fig. 5 (and Fig. S6 in the Supporting Material) it is evident that there are both spectral and kinetic changes in the PVB data over these timescales.
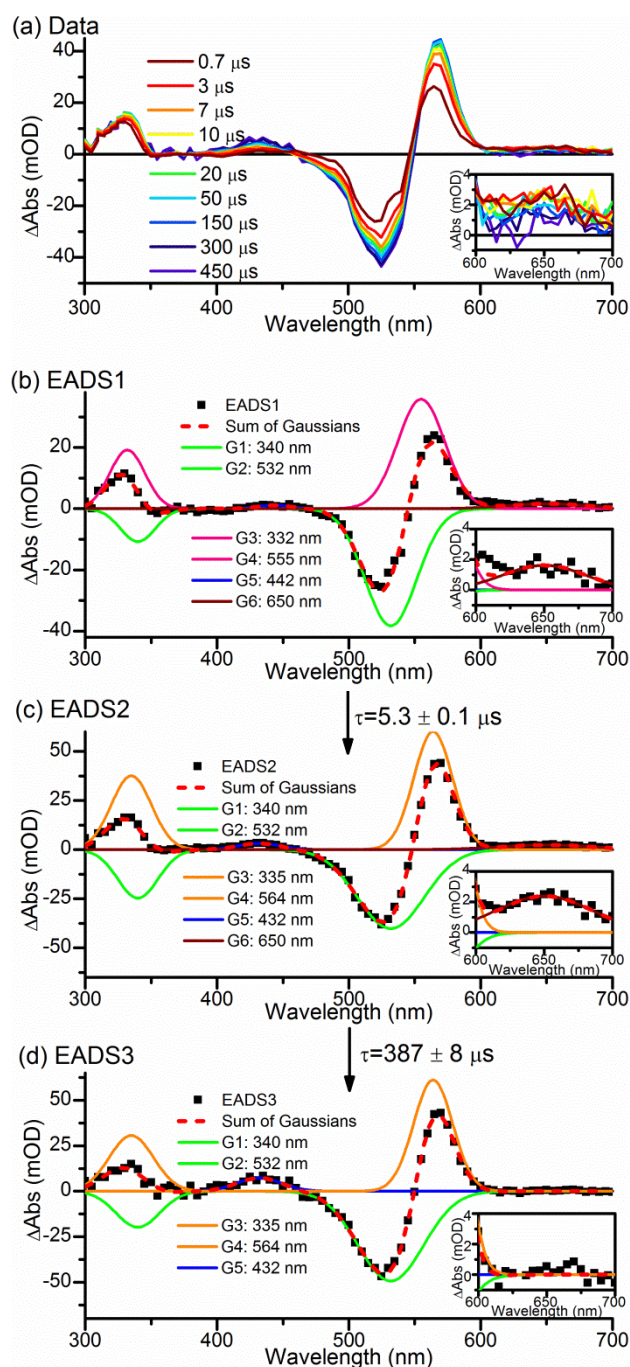
FIGURE 5 Transient absorption data of PVB Tlr0924 after excitation at 532 nm collected over 1 – 450 μs (a) and the EADS resulting from global analysis (black dots) fitted with a sum of Gaussian functions (dashed red). The features are assigned as: GSB of the PVB Pg state at 532 and 340 nm (green), the first intermediate at 555 and 332 nm (pink), and the second intermediate at 564 and 335 nm (orange). Insets show expanded 600 – 700 nm region containing 650 nm intermediate (maroon).

The sub-μs data-set did not show any additional features so the 1 – 450 μs data-set was analyzed using a sequential model (Fig. 5b-d). Three components were needed to completely describe the data. The first component, EADS1, is qualitatively similar to the SADS2 derived from the ultrafast visible TA measurements (Fig. 4b). The laser flash photolysis

measurements extend further into the UV, allowing further characterization of the various intermediates. The significant features present in both difference spectra are the ground state bleaches at 532 (and 340 nm), and the intermediate with a strong absorbance at 555 (and 332) nm. The less intense features do appear to be slightly different: 440, 496, 604 and 663 nm in the ultrafast data compared with 442 and 650 nm in the flash photolysis data. Any differences can be attributed to differences in the experimental techniques. Flash photolysis data will show all changes compared to a 'true' pre-excitation signal. In contrast the ultrafast visible and IR pump-probe measurements use a 1 or 10 kHz laser respectively, so data show changes compared to the sample 1 or 0.1 ms after excitation. EADS1 decays into EADS2 with a lifetime of 5.3 μs, and EADS3 grows in from EADS2 with a lifetime of 387 μs. The major spectral features of EADS2 and EADS3 are identical; the GSB features at 340 and 532 nm remain, but the intermediate features previously at 332 and 555 nm shift to 335 and 564 nm respectively. The difference between EADS2 and EADS3 is in the lower intensity features in the red region of the spectrum, which are present in the EADS2, but not EADS3, which may be due to a small proportion of PCB Pr to Pb conversion occurring in parallel to the much more intense PVB processes. The final intermediate in these data, with an absorption maximum at 564 nm corresponds exactly with the intermediate previously observed in non time-resolved studies, assigned by those studies to the isomerised but not yet thioether linked chromophore.(21, 23)

Millisecond to Second Transient Absorption

The final set of laser flash photolysis measurements on millisecond timescales monitored the final step in the photoconversion reaction, when the isomerised intermediate forms a thioether linkage with the Cys-499 residue in the protein. The PVB Pg population was isolated as described in the previous section. The data, shown in Fig. 6a, initially have the same features as those described in the final EADS of the ns to ms data-set. Over the course of a few ms this converts to the final state with a large positive feature at ~430 nm. The data fit well to a sequential model with only 2 components, which interconvert with a lifetime of 23.6 ms. The first EADS is essentially identical to EADS3 in Fig. 5d, with GSB of the Pg state at 340 and 532 nm, and the intermediate with features at 335 and 564 nm. EADS1 converts to the final difference spectra, EADS2, in which the GSB of the Pg state remain, and the final Pb state at 436 nm is apparent.
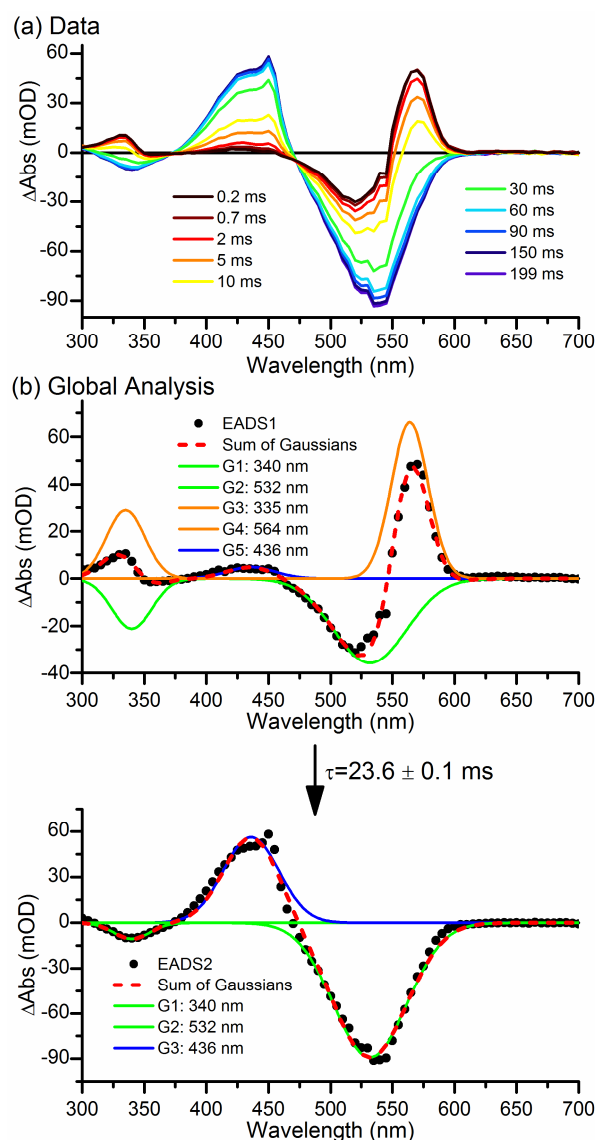
FIGURE 6 Transient absorption spectra of PVB Tlr0924 after excitation at 532 nm at selected time points over 0.2 – 199 ms (a), and global analysis of the data (b) showing the resulting EADS (black dots) fitted with a sum of Gaussian functions (red line). There are features originating from the bleach of the Pg state (green lines), the second intermediate (orange lines), and the final Pb state (blue lines).

Cryotrapping

To determine which of the transitions observed in the time-resolved measurements were thermally activated cryotrapping measurements were carried out. In these experiments a sample in the PVB Pg state was illuminated with a cold light source fitted with a 530 nm bandpass filter at 127 K, then warmed to 297 K in 10 K steps, with spectra collected at 99 K between each temperature point. Difference spectra relative to the 'dark spectrum' at 99 K are shown in Figs. 7a and b.
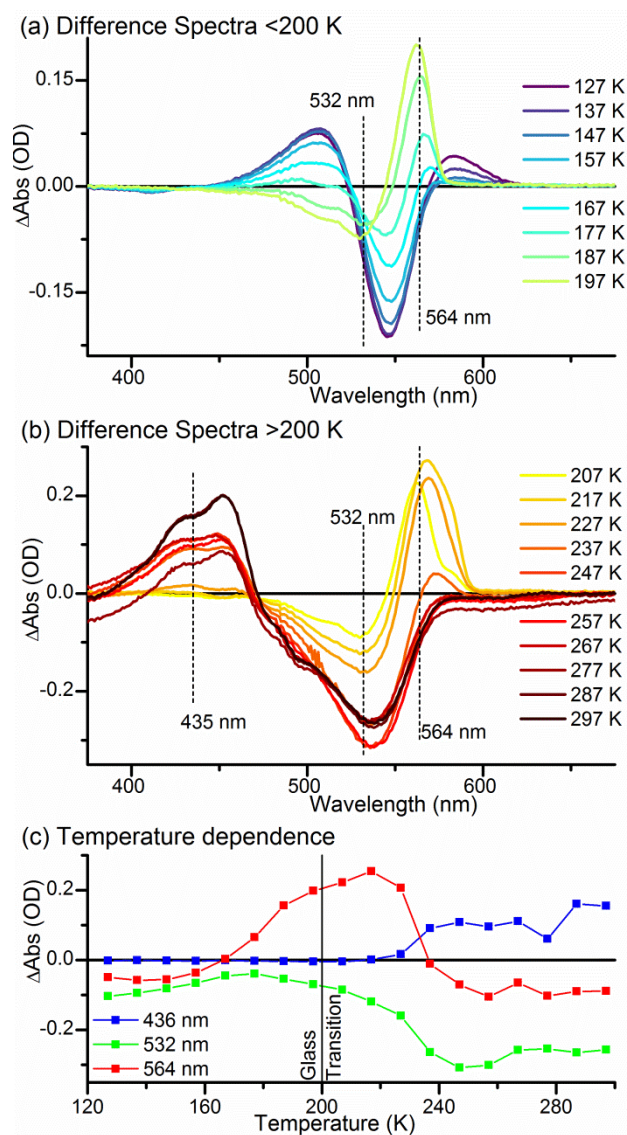
FIGURE 7 a) Difference spectra at selected temperatures relative to 'dark spectrum' at 99 K a) below 200 K and b) above 200 K. c) Temperature dependence of selected wavelengths over the 127 – 297 K temperature range.

The difference spectra in Fig. 7a show a number of intermediates being formed. Throughout the measurement the bleach of the ground state at ~530 nm is visible. At the lowest temperatures there are positive features visible at ~583 nm and ~506 nm which are lost at 157 and 177 K respectively. These two features are not observed in the time-resolved measurements, where the ground state bleach is significantly more intense due to the large excited state population. While the ~506 nm feature reduces in intensity as the sharp feature at ~560 nm appears, the ~583 nm peak does not seem to correlate with any other features. There are two most likely possible explanations for these features. They may be artefacts of the cryogenic techniques used; previous studies have shown that cryogenic temperatures can affect the energy landscape and possible conformational substates of proteins.(38-40) This variation in protein structure could in turn affect the absorption properties of the chromophore. The other option is that these features are true intermediates in the photoreaction which were not resolvable in the ultrafast measurements because of either their

very short lifetimes (<<0.6 ps) or low intensity relative to the very strong excited state features.

Above ~187 K (Fig. 7b) the spectral features in the cryotrapping data more closely resemble the features observed in the time-resolved data. The temperature dependent spectral evolution at selected wavelength points is displayed in Fig. 7c. It is not possible to resolve the 555 and 564 nm intermediates but the final step in the time-resolved data from the intermediate at 564 nm to the Pb state correlates very well with the final step observed in the cryotrapping measurements at 237 K. By fitting the temperature dependence at selected wavelengths (see Fig. S7 in the Supporting Material) it is possible to put the temperature of formation of the 555/564 nm intermediate at around 179 K, and the formation of the final product state at around 232 K. At ~200 K it is known that proteins undergo a dynamic transition, termed the 'glass transition', below which any large-scale conformational changes in the protein that require solvent reorganization become frozen out.(9, 41) As the formation of the 555/564 nm intermediate occurs close to this temperature it may be accompanied by some minor structural changes in the protein. However, the final transition to form the Pb state can only proceed well above this 'glass transition' temperature, demonstrating that more large-scale protein motions are likely to be required for this stage of the photoconversion. This is a similar picture to that observed in the forward reaction of Tlr0924 and the photoreaction of the related Cph1 phytochrome.(9, 20)

CONCLUSION

The time-resolved visible and IR transient absorption data described here present a clear picture of the PVB Pg to Pb photoconversion (Fig. 8). After photoexcitation of the PVB Pg state the majority of the excited state population relaxes back to the ground state with a lifetime of 0.6 ps. A small proportion of the excited population isomerises with a lifetime of 3.6 ps to the 15Z-PVB, with an absorption maxima at 555 nm. The final Pb state of the PVB' is linked by a thioether linkage to a Cys in the bulk protein structure. Before the formation of this linkage another step, with a lifetime of 5.3 µs, occurs to form a further intermediate absorbing at 564 nm. The structure of this intermediate is not certain but it involves a red-shift in the absorbance maxima at temperatures close to the 'glass transition' temperature of proteins. Hence, it is possible that it may involve some twisting or other structural distortion of the chromophore, assisted by protein motions in the binding pocket, in which it becomes more planar, delocalizing the π-orbital system, causing the red shift in absorbance maxima.(16) Similar intermediates have been suggested for a number of related phytochrome and CBCR systems.(16, 42-45) The final step of the reaction progresses with a lifetime of 23.6 ms to the final Cys-bound 15Z-Pb state and will likely involve some large-scale movement of the protein structure.
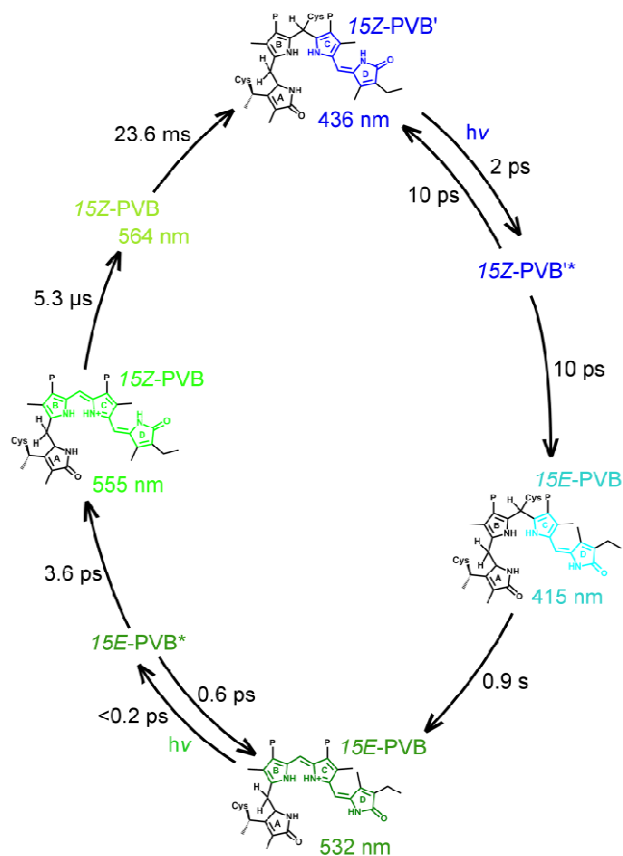
FIGURE 8 Suggested reaction scheme for the full PVB conversion cycle including details of both the Pg to Pb reaction from this work, and the Pb to Pg reaction.(20)

The time-resolved data presented here for μs to ms timescales are comparable to those reported for other CBCRs. Flash photolysis measurements have shown that the slower steps in the photoconversion process often proceed *via* 2-3 intermediates with spectrally distinct features. The precise nature of these intermediates is not confirmed, but isomerisation and changes in the localization of the π-orbital system are both suggested. There is quite a variation in the lifetimes of conversion between these intermediates. The final two steps can occur with lifetimes of ~1 μs and ~920 μs (AnPixJ),(16) 750 ns and >1 ms (NpF2164g3),(19) and 390 μs and 1.5 ms (Slr1393).(46) None of these lifetimes are as long as the 23.6 ms observed for the final reaction step reported here, even in the case of NpF2164g3 which, as with Tlr0924, forms two thioether linkages with the protein. However, these previous studies were on the GAF domain only system, whereas here we have investigated the full length protein, which may significantly extend the kinetics.(46)

The scheme suggested here is more complex than that suggested for the Pb to Pg forward reaction.(20) In that case there are simply 2 steps, the fast photoisomerisation followed by the very slow breakage of the thioether linkage. Neither of those steps depends strongly on the geometry and configuration of the chromophore ring systems. In contrast, in the reverse reaction after the photoisomerisation the chromophore must move into a geometry favourable for the formation of the thioether linkage, but overall the reaction progresses faster and is completed in ms, compared to seconds.

ACKNOWLEDGMENTS

REFERENCES

1. Ikeuchi, M., and T. Ishizuka. 2008. Cyanobacteriochromes: a new superfamily of tetrapyrrole-binding photoreceptors in cyanobacteria. *Photoch. Photobio. Sci.* 7:1159-1167.

2. Narikawa, R., T. Ishizuka, N. Muraki, T. Shiba, G. Kurisu, and M. Ikeuchi. 2013. Structures of cyanobacteriochromes from phototaxis regulators AnPixJ and TePixJ reveal general and specific photoconversion mechanism. *P. Natl. Acad. Sci. USA* 110:918-923.

3. Hirose, Y., N. C. Rockwell, K. Nishiyama, R. Narikawa, Y. Ukaji, K. Inomata, J. C. Lagarias, and M. Ikeuchi. 2013. Green/red cyanobacteriochromes regulate complementary chromatic acclimation via a protochromic photocycle. *P. Natl. Acad. Sci. USA* 110:4974-4979.

4. Rockwell, N. C., S. S. Martin, K. Feoktistova, and J. C. Lagarias. 2011. Diverse two-cysteine photocycles in phytochromes and cyanobacteriochromes. *P. Natl. Acad. Sci. USA* 108:11854-11859.

5. Sun, Y.-F., J.-G. Xu, K. Tang, D. Miao, W. Gärtner, H. Scheer, K.-H. Zhao, and M. Zhou. 2014. Orange fluorescent proteins constructed from cyanobacteriochromes chromophorylated with phycoerythrobilin. *Photoch. Photobio. Sci.* 13:757-763.

6. Pathak, G. P., J. D. Vrana, and C. L. Tucker. 2012. Optogenetic control of cell function using engineered photoreceptors. *Biol. Cell* 105:59-72.

7. Zhou, J., and Y. Li. 2010. Engineering cyanobacteria for fuels and chemicals production. *Protein and Cell* 1:207-210.

8. Linke, M., Y. Yang, B. Zienicke, M. A. S. Hammam, T. von Haimberger, A. Zacarias, K. Inomata, T. Lamparter, and K. Heyne. 2013. Electronic transitions and heterogeneity of the bacteriophytochrome Pr absorption band: An angle balanced polarization resolved femtosecond VIS pump-IR probe study. *Biophys. J.* 105:1756-1766.

9. Heyes, D. J., B. Khara, M. Sakuma, S. J. O. Hardman, R. O'Cualain, S. E. J. Rigby, and N. S. Scrutton. 2012. Ultrafast Red Light Activation of Synechocystis Phytochrome Cph1 Triggers Major Structural Change to Form the Pfr Signalling-Competent State. *PLoS One* 7:e52418.

10. Müller, M. G., I. Lindner, I. Martin, W. Gärtner, and A. R. Holzwarth. 2008. Femtosecond kinetics of photoconversion of the higher plant photoreceptor phytochrome carrying native and modified chromophores. *Biophys. J.* 94:4370-4382.

11. Heyne, K., J. Herbst, D. Stehlik, B. Esteban, T. Lamparter, J. Hughes, and R. Diller. 2002. Ultrafast dynamics of phytochrome from the cyanobacterium Synechocystis, reconstituted with phycocyanobilin and phycoerythrobilin. *Biophys. J.* 82:1004-1016.

12. Gottlieb, S. M., P. W. Kim, N. C. Rockwell, Y. Hirose, M. Ikeuchi, J. C. Lagarias, and D. S. Larsen. 2013. Primary Photodynamics of the Green/Red-Absorbing Photoswitching

Regulator of the Chromatic Adaptation E Domain from Fremyella diplosiphon. *Biochemistry* 52:8198-8208.

13. Bischoff, M., G. Hermann, S. Rentsch, and D. Strehlow. 2001. First steps in the phytochrome phototransformation: A comparative femtosecond study on the forward (Pr -> Pfr) and back reaction (Pfr -> Pr). *Biochemistry* 40:181-186.

14. Kim, P. W., L. H. Freer, N. C. Rockwell, S. S. Martin, J. C. Lagarias, and D. S. Larsen. 2012. Femtosecond Photodynamics of the Red/Green Cyanobacteriochrome NpR6012g4 from Nostoc punctiforme. 2. Reverse Dynamics. *Biochemistry* 51:619-630.

15. Burgie, E. S., J. M. Walker, G. N. Phillips, Jr., and R. D. Vierstra. 2013. A Photo-Labile Thioether Linkage to Phycoviolobilin Provides the Foundation for the Blue/Green Photocycles in DXCF-Cyanobacteriochromes. *Structure* 21:88-97.

16. Fukushima, Y., M. Iwaki, R. Narikawa, M. Ikeuchi, Y. Tomita, and S. Itoh. 2011. Photoconversion Mechanism of a Green/Red Photosensory Cyanobacteriochrome AnPixJ: Time-Resolved Optical Spectroscopy and FTIR Analysis of the AnPixJ-GAF2 Domain. *Biochemistry* 50:6328-6339.

17. Piwowarski, P., E. Ritter, K.-P. Hofmann, P. Hildebrandt, D. von Stetten, P. Scheerer, N. Michael, T. Lamparter, and F. Bartl. 2010. Light-Induced Activation of Bacterial Phytochrome Agp1 Monitored by Static and Time-Resolved FTIR Spectroscopy. *ChemPhysChem* 11:1207-1214.

18. Freer, L. H., P. W. Kim, S. C. Corley, N. C. Rockwell, L. Zhao, A. J. Thibert, J. C. Lagarias, and D. S. Larsen. 2012. Chemical Inhomogeneity in the Ultrafast Dynamics of the DXCF Cyanobacteriochrome Tlr0924. *J. Phys. Chem. B* 116:10571-10581.

19. Gottlieb, S. M., P. W. Kim, S. C. Corley, D. Madsen, S. J. Hanke, N. C. Rockwell, C.-W. Chang, S. S. Martin, J. C. Lagarias, and D. S. Larsen. 2014. Primary and Secondary Photodynamics of the Violet/Orange Dual-Cysteine NpF2164g3 Cyanobacteriochrome Domain from Nostoc Punctiforme. *Biochemistry* 53:1029-1040.

20. Hauck, A. F. E., S. J. O. Hardman, R. J. Kutta, G. M. Greetham, D. J. Heyes, and N. S. Scrutton. 2014. An unprecedented long photoconversion over twelve orders of magnitude for full-length cyanobacteriochrome Tlr0924. *J. Biol. Chem.* 289:17747-17757.

21. Rockwell, N. C., S. L. Njuguna, L. Roberts, E. Castillo, V. L. Parson, S. Dwojak, J. C. Lagarias, and S. C. Spiller. 2008. A second conserved GAF domain cysteine is required for the blue/green photoreversibility of cyanobacteriochrome Tlr0924 from Thermosynechococcus elongatus. *Biochemistry* 47:7304-7316.

22. Enomoto, G., R. Nomura, T. Shimada, W. Ni Ni, R. Narikawa, and M. Ikeuchi. 2014. Cyanobacteriochrome SesA Is a Diguanylate Cyclase That Induces Cell Aggregation in Thermosynechococcus. *J. Biol. Chem.* 289:24801-24809.

23. Rockwell, N. C., S. S. Martin, A. G. Gulevich, and J. C. Lagarias. 2012. Phycoviolobilin Formation and Spectral Tuning in the DXCF Cyanobacteriochrome Subfamily. *Biochemistry* 51:1449-1463.

24. Ishizuka, T., A. Kamiya, H. Suzuki, R. Narikawa, T. Noguchi, T. Kohchi, K. Inomata, and M. Ikeuchi. 2011. The Cyanobacteriochrome, TePixJ, Isomerizes Its Own Chromophore by Converting Phycocyanobilin to Phycoviolobilin. *Biochemistry* 50:953-961.

25. Rockwell, N. C., Y. S. Su, and J. C. Lagarias. 2006. Phytochrome structure and signaling mechanisms. *Annu. Rev. Plant Biol.* 57:837-858.

26. Greetham, G. M., P. Burgos, Q. A. Cao, I. P. Clark, P. S. Codd, R. C. Farrow, M. W. George, M. Kogimtzis, P. Matousek, A. W. Parker, M. R. Pollard, D. A. Robinson, Z. J. Xin, and M. Towrie. 2010. ULTRA: A Unique Instrument for Time-Resolved Spectroscopy. *Appl. Spectrosc.* 64:1311-1319.

27. Jones, A. R., H. J. Russell, G. M. Greetham, M. Towrie, S. Hay, and N. S. Scrutton. 2012. Ultrafast Infrared Spectral Fingerprints of Vitamin B-12 and Related Cobalamins. *J. Phys. Chem. A* 116:5586-5594.

28. Snellenburg, J. J., S. P. Laptenok, R. Seger, K. M. Mullen, and I. H. M. van Stokkum. 2012. Glotaran: A Java-Based Graphical User Interface for the R Package TIMP. *J. Stat. Softw.* 49:1-22.

29. Lorenc, M., M. Ziolek, R. Naskrecki, J. Karolczak, J. Kubicki, and A. Maciejewski. 2002. Artifacts in femtosecond transient absorption spectroscopy. *Appl. Phys. B: Lasers Opt.* 74:19-27.

30. Salewski, J., F. V. Escobar, S. Kaminski, D. von Stetten, A. Keidel, Y. Rippers, N. Michael, P. Scheerer, P. Piwowarski, F. Bartl, N. Frankenberg-Dinkel, S. Ringsdorf, W. Gärtner, T. Lamparter, M. A. Mroginski, and P. Hildebrandt. 2013. Structure of the Biliverdin Cofactor in the Pfr State of Bathy and Prototypical Phytochromes. *J. Biol. Chem.* 288:16800-16814.

31. Mroginski, M. A., F. Mark, W. Thiel, and P. Hildebrandt. 2007. Quantum Mechanics/Molecular Mechanics Calculation of the Raman Spectra of the Phycocyanobilin Chromophore in α-C-Phycocyanin. *Biophys. J.* 93:1885-1894.

32. Dasgupta, J., R. R. Frontiera, K. C. Taylor, J. C. Lagarias, and R. A. Mathies. 2009. Ultrafast excited-state isomerization in phytochrome revealed by femtosecond stimulated Raman spectroscopy. *P. Natl. Acad. Sci. USA* 106:1784-1789.

33. Toh, K. C., E. A. Stojkovic, A. B. Rupenyan, I. H. M. van Stokkum, M. Salumbides, M.-L. Groot, K. Moffat, and J. T. M. Kennis. 2011. Primary Reactions of Bacteriophytochrome Observed with Ultrafast Mid-Infrared Spectroscopy. *J. Phys. Chem. A* 115:3778-3786.

34. van Thor, J. J., K. L. Ronayne, and M. Towrie. 2007. Formation of the early photoproduct Lumi-R of cyanobacterial phytochrome Cph1 observed by ultrafast mid-infrared spectroscopy. *J. Am. Chem. Soc.* 129:126-132.

35. Mirkovic, T., A. B. Doust, J. Kim, K. E. Wilk, C. Curutchet, B. Mennucci, R. Cammi, P. M. G. Curmi, and G. D. Scholes. 2007. Ultrafast light harvesting dynamics in the cryptophyte phycocyanin 645. *Photoch. Photobio. Sci.* 6:964-975.

36. Zehetmayer, P., M. Kupka, H. Scheer, and A. Zumbusch. 2004. Energy transfer in monomeric phycoerythrocyanin. *BBA-Bioenergetics* 1608:35-44.

37. Rockwell, N. C., S. S. Martin, and J. C. Lagarias. 2012. Red/Green Cyanobacteriochromes: Sensors of Color and Power. *Biochemistry* 51:9667-9677.

38. Anderson, S., V. Šrajer, and K. Moffat. 2004. Structural Heterogeneity of Cryotrapped Intermediates in the Bacterial Blue Light Photoreceptor, Photoactive Yellow Protein. *Photochem. Photobiol.* 80:7-14.

39. Frauenfelder, H. 2010. Proteins, supercooled liquids, and glasses: A micro-review. *Physica E* 42:662-665.

40. Lubchenko, V., P. G. Wolynes, and H. Frauenfelder. 2005. Mosaic Energy Landscapes of Liquids and the Control of Protein Conformational Dynamics by Glass-Forming Solvents. *J. Phys. Chem. B* 109:7488-7499.

41. Vitkup, D., D. Ringe, G. A. Petsko, and M. Karplus. 2000. Solvent mobility and the protein 'glass' transition. *Nat. Struct. Biol.* 7:34-38.

42. Yoshihara, S., T. Shimada, D. Matsuoka, K. Zikihara, T. Kohchi, and S. Tokutomi. 2006. Reconstitution of blue-green reversible photoconversion of a cyanobacterial photoreceptor, PixJ1, in phycocyanobilin-producing Escherichia coli. *Biochemistry* 45:3775-3784.

43. Matysik, J., P. Hildebrandt, W. Schlamann, S. E. Braslavsky, and K. Schaffner. 1995. Fourier-Transform Resonance Raman Spectroscopy of Intermediates of the Phytochrome Photocycle. *Biochemistry* 34:10497-10507.

44. Foerstendorf, H., C. Benda, W. Gärtner, M. Storf, H. Scheer, and F. Siebert. 2001. FTIR studies of phytochrome photoreactions reveal the C=O bands of the chromophore: Consequences for its protonation states, conformation, and protein interaction. *Biochemistry* 40:14952-14959.

45. Rockwell, N. C., S. S. Martin, A. G. Gulevich, and J. C. Lagarias. 2014. Conserved Phenylalanine Residues Are Required for Blue-Shifting of Cyanobacteriochrome Photoproducts. *Biochemistry* 53:3118–3130.

46. Xu, X.-L., A. Gutt, J. Mechelke, S. Raffelberg, K. Tang, D. Miao, L. Valle, C. D. Borsarelli, K.-H. Zhao, and W. Gärtner. 2014. Combined Mutagenesis and Kinetics Characterization of the Bilin-Binding GAF Domain of the Protein Slr1393 from the Cyanobacterium Synechocystis PCC6803. *ChemBioChem* 15:1190-1199.

SUPPORTING MATERIAL

Fig. S1. Ultrafast transient absorption data collected with depolarised pump beam, Fig. S2. Cryotrapping experiments where the sample was warmed from 77 K in 10 K steps, illuminating at each temperature, Fig. S3. Ultrafast transient absorption data and global analysis showing the low intensity components after ~20ps, Fig. S4. SVD of residual from global analysis of ultrafast transient absorption data, Figure. S5 Sequential global analysis of the ultrafast visible transient absorption data showing resulting EADS fitted with a sum of Gaussian functions, Fig. S6 Laser flash photolysis data collected with PVB Tlr0924 after excitation at 532 nm, Fig.S7 Fitting of temperature dependence of absorption features are available at: www.biophys.org/biophysj/supplemental/S0006-3495(XX)XXXXX-X.

FIGURE TITLES AND LEGENDS

FIGURE 1 Structures and absorption spectra of the PCB and PVB photostates. The PCB and PVB chromophores can interconvert by autoisomerization, the ^{15Z}Pb and ^{15E}Pg and ^{15E}Pr states can reversibly photoconvert.

FIGURE 2 Ultrafast visible transient absorption spectra at selected time points (a), and the EADS resulting from a sequential global analysis of the data (b). The sample was constantly illuminated during data collection with blue and red light so the signals primarily originate from the Pg to Pb photoconversion of the PVB chromophore.

FIGURE 3 Ultrafast IR transient absorption spectra at selected time points (a), and the EADS resulting from a sequential global analysis of the data (b). The sample was constantly illuminated during data collection with blue and red light so the signals primarily originate from the Pg to Pb photoconversion of the PVB chromophore

FIGURE 4 Global analysis of the ultrafast visible (a-c) and IR (d-f) transient absorption data showing resulting SADS (black). The visible TA SADS are fitted with a sum of Gaussian functions (dashed red). The features of SADS1 (a) and SADS2(b) are assigned as: GSB of the PVB Pg state at 532 nm (green), ESA features at 440, 496, and 663 nm (lilac, cyan and orange), intermediate states at 550, 604, and 648nm (pink), and pump scatter at 525 nm (grey). SADS3, representing inactive or modified protein has additional peaks at 641 nm (dark green) and 581 nm (purple).

FIGURE 5 Transient absorption data of PVB Tlr0924 after excitation at 532 nm collected over $1 - 450$ μs (a) and the EADS resulting from global analysis (black dots) fitted with a sum of Gaussian functions (dashed red). The features are assigned as: GSB of the PVB Pg state at 532 and 340 nm (green), the first intermediate at 555 and 332 nm (pink), and the second intermediate at 564 and 335 nm (orange). Insets show expanded $600 - 700$ nm region containing 650 nm intermediate (maroon).

FIGURE 6 Transient absorption spectra of PVB Tlr0924 after excitation at 532 nm at selected time points over $0.2 - 199$ ms (a), and global analysis of the data (b) showing the resulting EADS (black dots) fitted with a sum of Gaussian functions (red line). There are features originating from the bleach of the Pg state (green lines), the second intermediate (orange lines), and the final Pb state (blue lines).

FIGURE 7 a) Difference spectra at selected temperatures relative to 'dark spectrum' at 99 K a) below 200 K and b) above 200 K. c) Temperature dependence of selected wavelengths over the $127 - 297$ K temperature range.

FIGURE 8 Suggested reaction scheme for the full PVB conversion cycle including details of both the Pg to Pb reaction from this work, and the Pb to Pg reaction.